Status of the ATLAS Experiment and Early Physics Measurements

Mauro Iodice[a]

On behalf of the ATLAS Collaboration

INFN Sezione di Roma Tre, Via della Vasca Navale, 84 - 00146 - Rome, Italy

Abstract. The ATLAS experiment has collected several hundred million cosmic ray events during 2008 and 2009 providing the primary source for commissioning the detectors, trigger, data acquisition and event reconstruction programs. The data allowed studying the performance of all detector components. Results on performance and readiness of the sub-detectors will be reported. We will also outline the potential for early physics measurements during the first year of operation.

1 The ATLAS Experiment at the Large Hadron Collider

ATLAS is a multipurpose detector [1] installed at the Large Hadron Collider (LHC) at CERN where two proton beams collide at a design center-of-mass-energy of 14 TeV. After many years of design, constructions and installation, the first beams were circulated on September 10th 2008. Unfortunately an incident occurred about a week later and, as a consequence, a long shutdown period was planned. The ATLAS collaboration made profit of the shutdown by undertaking a variety of maintenance, consolidation and repair work on the detector as well as major runs with cosmic rays. In the past two years many cosmic ray data have been collected and provided the primary source for commissioning all systems of the experiment.

The commissioning and performance studies of the challenging detection technologies composing the detector, are presented, along with the potential for early physics measurements during the first year of operation.

The aim of the experiment to explore physics up to the TeV scale with proton–proton collisions at 14 TeV in the center of mass, at a design luminosity of $10^{34} \text{cm}^{-2}\text{s}^{-1}$ with a bunch crossing rate of 40 MHz. The design performance, validated by a long campaign of test beam measurements and detailed Monte Carlo simulations is summarized in [2]. At the LHC the production of QCD jets overwhelm interesting rare physics signatures which can be tagged by the presence of leptons. With the total inelastic cross-section $\sigma_{inel} \sim 80$ mb, the rate of inelastic events will be $\sim 10^9$ Hz. This should be compared with the rate of interesting processes, such as W-boson leptonic decay $W \to l\nu$, 200 Hz, $t\bar{t}$ production, 8 Hz, or Higgs boson production, 0.6 Hz (0.02 Hz) for $M_H = 100$ (600) GeV.

1.1 Detector Design and Requirements

The ATLAS detector [3] is designed to have excellent tracking, calorimetry and high resolution lepton detection over the entire range of energy accessible at the LHC. Clear identification and precise measurements of muons and electrons with high jet-rejection factor ($\mathcal{O}(10^6)$ at $p_T \sim 20$ GeV) is a requirement to the detectors.

---

[a] e-mail: `mauro.iodice@roma3.infn.it`
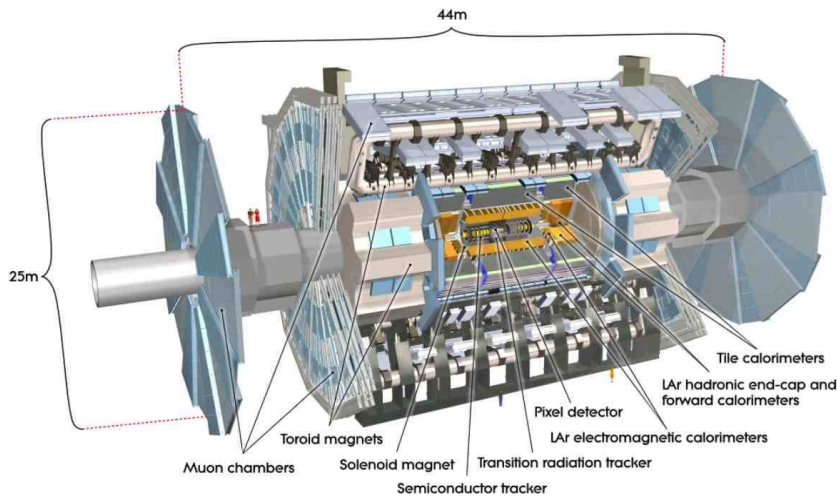
Fig. 1. A schematic view of the ATLAS detector.

The trigger selectivity should reduce the event rate to about 200 Hz from the bunch crossing rate of 40 MHz. A trigger system in three levels is adopted: Level-1 trigger is implemented by hardware with a fixed latency of 2.5 μs and a maximum output rate of 75 kHz, the level-2 and event filter have software implementation with approximate output rate of 2 kHz and 200 Hz, and average processing time of 40 ms and 4 s, respectively.

Essential characteristics of the ATLAS detector include: good tracking and vertex resolution; high hermeticity, with calorimetric coverage up to $|\eta| = 5$ for high resolution measurements of jet energy and missing transverse energy (E_T); very good electromagnetic calorimetry for electron and photon identification complemented by a Transition Radiation Tracker; high resolution and wide acceptance muon measurement with a standalone system, the Muon Spectrometer.

A schematic view of the ATLAS detector is shown in Fig. 1. It has a cylindrical shape of 44 m in length along the beam line and 25 m in diameter.

The innermost part is the Inner Detector (ID) made of three major components: the Pixel detector, the Semi-Conductor Tracker (SCT) and the Transition Radiation Tracker (TRT). The ID is operated in an axial 2 Tesla magnetic field and has a design momentum resolution of $\sigma(p_T)/p_T = 0.05\% \times p_T/\mathrm{GeV} \oplus 1\%$ ($\sim$5% at 100 GeV) and an impact parameter resolution $\sigma(d_0) = 10\mu\mathrm{m} \oplus 140\mu\mathrm{m}/(p_T/\mathrm{GeV})$. The TRT allows electron–pion separation over the energy range of 0.5–150 GeV.

Around the superconducting solenoid, containing the ID, is the calorimeter made of two types of sampling technologies: the Liquid Argon Calorimeter (LAr) in accordion geometry, and the Tile Calorimeter made of scintillator tiles and iron absorber. Electromagnetic calorimetry is realized with LAr technology with lead absorber in the barrel and the end-caps. Its energy resolution is $\sigma/E = 10\%/\sqrt{E/\mathrm{GeV}} \oplus 0.7\%$. Hadronic calorimetry uses Tiles in the barrel, with an energy resolution of $\sigma/E = 50\%/\sqrt{E/\mathrm{GeV}} \oplus 3\%$ for $|\eta| < 3.2$, and LAr in the end-caps, with a resolution of $\sigma/E = 100\%/\sqrt{E/\mathrm{GeV}} \oplus 10\%$ in the rapidity range $3.1 < |\eta| < 4.9$.

The outermost part is the Muon Spectrometer (MS) with momentum resolution of less than 5% for $p_T < 300$ GeV and $\sim$10% at 1 TeV. The magnetic field is generated by a system of three superconducting toroids in air, one for barrel and one for each of the end-caps.

For most of the acceptance the precision tracking chambers consist of Monitored Drift Tubes (MDT). In the end-cap inner regions, the Cathode Strip Chambers (CSC) are used since they are able to cope with higher background rates. The trigger chambers are based on two technologies: the Resistive Plate Chambers (RPC) instrument the barrel while the Thin Gap Chambers (TGC) are used in the higher background environment of the end-cap. Precision chambers should measure the muon position in the bending plane with an accuracy better than 40 μm to achieve the design momentum resolution.

2 Commissioning of the Detector Components and Results with Cosmic Data

A series of technical runs with cosmic rays were carried out to operate together the various sub-systems, to test the trigger and data acquisition systems, the Detector Control System (DCS, monitoring the status and parameters of operations), the data transfer and the data processing. The cosmic runs were also aimed at studying the detector performance and to validate the calibration tools and the alignment methods.

2.1 Inner Detector

The Pixel detector consists of three layers of pixels both in the barrel and in the end-cap regions, for a total of 80 million channels, with the innermost layer located at 5 cm distance from the beam line. The design values of the spatial resolution are 10 μm in the bending plane (R-Φ) and 115 μm in the beam direction (z). The SCT consists of 4 (9) double layers of silicon strips in the barrel (end-cap) with a spatial resolution of 17 μm (R-Φ) and 580 μm (z in the barrel, or R in the end-caps).

In order to match the required performance in tracking and momentum resolution, the position (alignment) of the Pixel and SCT modules must be known with an accuracy of a few microns. With samples of cosmic rays data, the track based detector alignment is performed using an iterative procedures that minimizes the hit residuals (distance between the hit and the reconstructed track). In Fig. 2 the hit residuals distribution in the precision coordinate is reported integrated over all hits-on-tracks in the barrel Pixel detector for the nominal geometry and the preliminary aligned geometry. The large width of the distribution for the nominal geometry reflects the level of accuracy of the positioning of the detector in ATLAS. For the aligned geometry the measured width of 24 μm is already close to the value of 16 μm from simulations of cosmics data.

The TRT detector is composed of 4 mm diameter straw tube layers, interleaved with transition radiation material allowing for e-π identification in the range 0.5 − 150 GeV. In the barrel region the tubes are assembled in 73 layers, parallel to the beam. Each of the end-cap TRT is composed of 160 layers of radial tubes (perpendicular to the beam). Studies on the transition radiation produced when a charged particle crosses the boundaries of two materials with different dielectric constants, have been carried out with cosmic muons in the TRT detector. In Fig. 3 one can see the turn-on of the production of TR photons as a function of Lorentz gamma as measured for the tracks of cosmic particles (muons). The data points represent the probability of a high-threshold hit (indicator for TR photons producing larger energy deposition in the straw tobes of the TRT). Measurements for both muon charges are compared with the results obtained in the ATLAS Combined Test Beam in 2004.

2.2 Calorimeters

The electromagnetic (EM) and hadronic calorimeters have been fully commissioned with cosmic rays and the response to minimum ionizing particles has been studied and compared with results from beam tests and simulations. The fraction of operational channels is more than 99.5% for all systems.

An example of the calorimeters responses to cosmic rays is shown in Fig. 4 and Fig. 5. Fig. 4 shows the response of the LAr (EM) calorimeter. Data are shown for the most probable energy as a function of pseudo-rapidity, along with the results from a simulation. The uniformity of the response agrees with simulation within 1% and the η dependence reflects the cell depth as one would expect for minimum ionizing particles.

The Tile calorimeter, performing the hadronic calorimetry in the barrel region, consists of scintillator tiles and iron absorber with 3 longitudinal samples. All calibration system, based on cesium sources, laser and charge injection, are operational. In Fig. 5 the response of the first layer cells as a function of η is shown. Vertical dashed lines correspond to the nominal
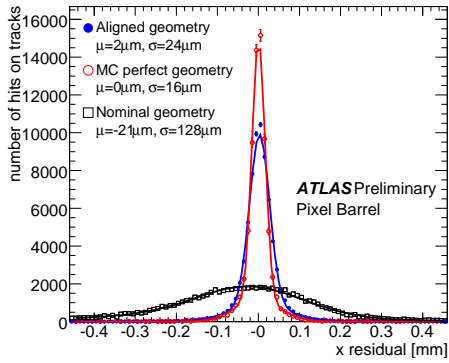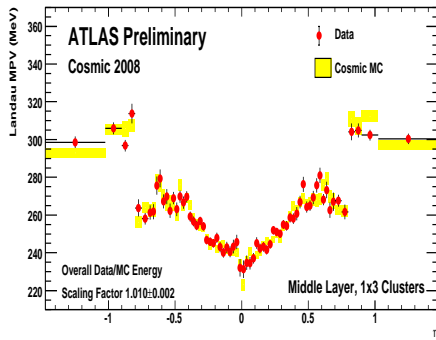
Fig. 2. Pixel hit residuals distribution in the precision coordinate for the nominal geometry and the preliminary aligned geometry.
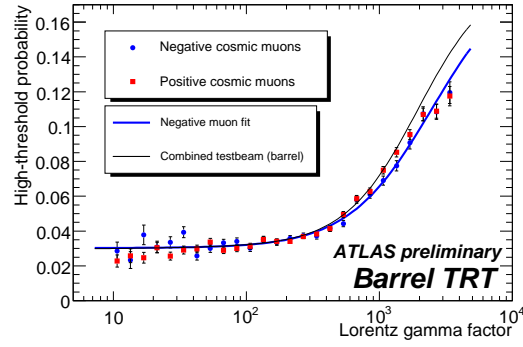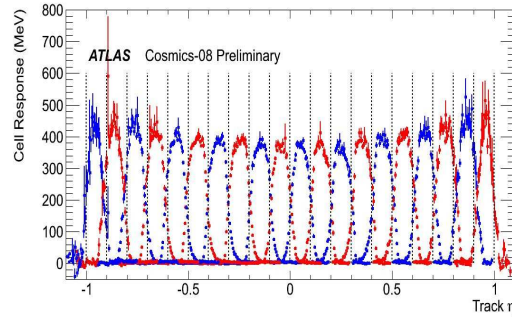

Fig. 3. Turn-on of the production of TR photons as a function of gamma as measured with cosmic rays.

position of the cell edges. The cell response is slightly increased at larger eta values because of the increasing muon path length.

Fig. 4. Resopnse for the middle layer of the LAr calorimeter to minimum ionizing particles as a function of η.


Fig. 5. Cell response of Tile calorimeter cells as a function of η.

2.3 Muon Spectrometer

The four technologies adopted in the MS have been fully commissioned and a fraction of channels very close to 100% is operational for MDT and TGC, and more than 97% and 98% for RPC and CSC, respectively.

The performance of the trigger chambers, RPC and TGC, have been studied in terms of detector coverage, timing, noise rate and efficiency. The efficiency for TGC layers has been evaluated asking a trigger coincidence of 3 out of 4 layers, thus not including the layer under observation in the trigger. An example of efficiency map for one layer of a TGC is reported in the left panel of Fig. 6. The right panel shows the efficiency projection onto the strip channel. Observed efficiency drops are consistent with wire support location. The efficiency measured in the active area ($\sim$99%) is in good agreement with dedicated tests before installation.
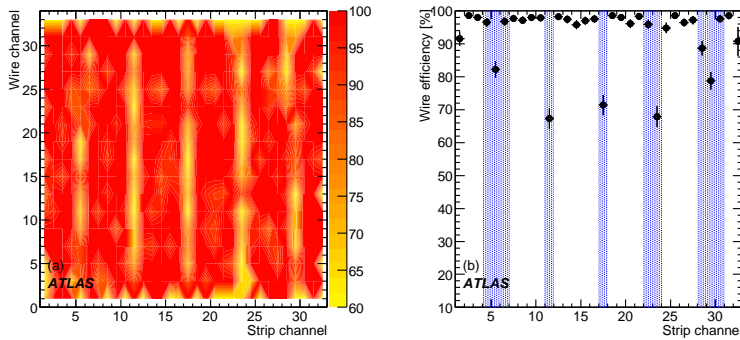
Fig. 6. Left: efficiency map for one layer of a TGC chamber; strip number on the horizontal axis, wire-group number on the vertical axis. Right: Efficiency projection onto the strip number. Regions of lower efficiency correspond to the wire supports (blue bands).

The MDT chambers have been extensively studied to optimize calibration procedures and tracking algorithms. The run conditions are different from those of the beam collisions: cosmic rays are not synchronous with the front-end electronics clock and are not pointing to the collision vertex. Single tube resolution has been measured as a function of the drift radius. The result, shown in Fig. 7, is compatible with that obtained with a high energy muon beam [4] if a degradation in timing resolution of about 2 ns is considered. This is due to the accuracy in the trigger jitter timing corrections, in addition to minor effects, among which, the multiple scattering of low momentum cosmic rays. An average spatial resolution of about 100 μm has been obtained. The efficiency has been measured for about 80,000 tubes in the barrel, for which sufficient statistics was collected. An average tracking efficiency of 95% at 5σ (fraction of hits with a distance from the segment within 5 times the position resolution) has been obtained. The result is shown in Fig. 8. About 0.2% of the channels are not functional and have an efficiency compatible with zero.
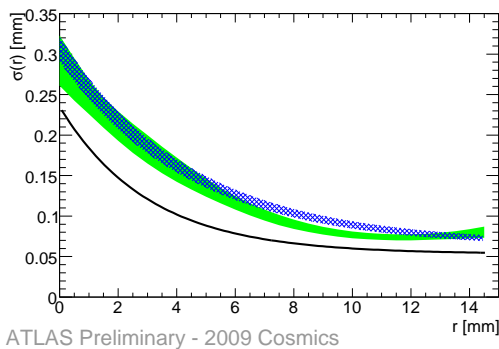

Fig. 7. Drift tube resolution as a function of the radius. The green and blue bands represent the resolution measured on cosmic ray samples with two different methods with the associated systematic error. The solid line represent the resolution measured in previous test beam.
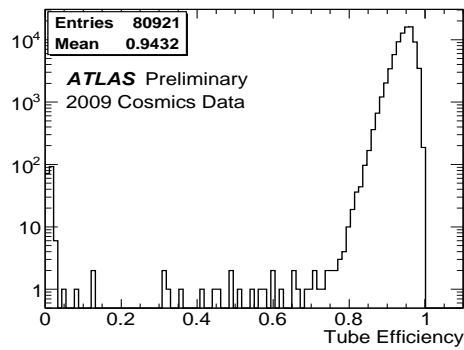
Fig. 8. MDT single-tube 5-sigma tracking efficiencies for about 80 thousand barrel channels.

Studies on the sagitta resolutions and the momentum resolution of the MS have been carried out. To reach the design p_T resolution the MDT chamber position need to be monitored with precisions better than ~ 40 μm, along distances of several meters. An alignment optical system is implemented in the MS allowing for a relative monitoring of chamber displacements to a 40 μm accuracy on the sagitta. However, to achieve the required absolute precision, a track-based alignment method has been implemented. In the end-cap region, the optical alignment system alone gives ~ 50 μm saggita accuracy. Cosmic ray data shows consistent result within statistical uncertainty. In the barrel region, only an absolute alignment accuracy of ~ 200 μm has been achieved so far due to design flaws. But with using cosmic tracks better than 100 μm accuracy has been measured, limited by statistics of pointing tracks.

With long tracks traversing the upper and lower regions of the barrel toroid it is possible to estimate the momentum scale and the momentum resolution. These tracks are measured twice while, in between, they traverse twice the barrel calorimeter. The difference of measured momenta is in fair agreement with the energy loss in the calorimeter. Taking this into account, the ratio of the difference to the average value is used to evaluate the momentum resolution. The resolution, shown in Fig. 9, is compatible with the predicted resolution for transverse momenta below 100 GeV and is degraded at higher momenta. This degradation is caused by imperfect alignment of the muon chambers and limited timing accuracy.
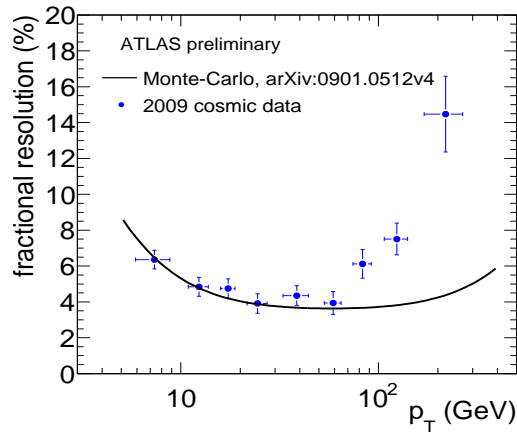

Fig. 9. Relative momentum resolution measured by comparing top and bottom MS tracks.

With data taken when the solenoid and the toroids were both "on", the correlation between the MS and the ID track parameters has been studied for tracks crossing both systems. Fig. 10 shows the correlation between the reconstructed azimuthal angles. The correlation shows that the ID and the MS both are well synchronized and aligned. Differences are in agreement with the effect of multiple scattering. Fig. 11 shows the difference in the momentum measured in the two systems. The measured shift is in good agreement with the estimated energy loss in the calorimeter.

3 Early Physics Measurements

The LHC start-up scenario foresees the first injection of proton beams in mid November 2009, the first collisions at the injection energy (450 GeV per beam) and eventually ramping up the beam energy to 1 TeV, before the end of the year. After a short Christmas shutdown the energy will be increased up to 3.5 TeV per beam with the goal of integrating 200 pb^{-1} in 2010. In this framework the main goal for ATLAS is to "calibrate" the detectors with measuring the main Standard Model (SM) processes. The properties of W, Z and top-quark will be
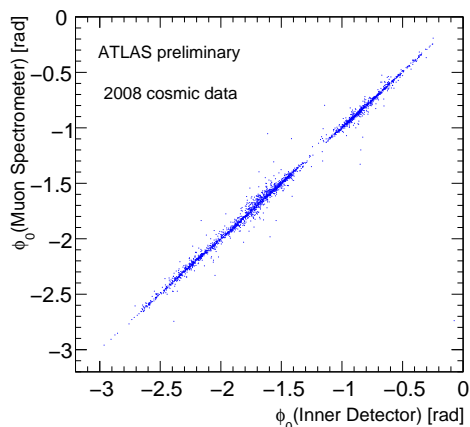
Fig. 10. Correlation between the ϕ angle measured in the MS and the ID.
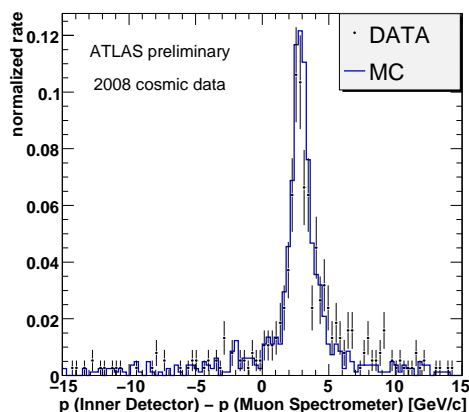

**Fig. 11.** Difference of momentum measured in the MS and in the ID.

accurately studied as they can be considered as benchmarks to assess the comprehension of the measurements. In the year to come, the most urgent goals are:

– Commissioning the detectors and triggers in collision mode and tuning the software tools, at the beginning with minimum bias events, di-lepton distributions (J/Ψ, Υ), inclusive muons and QCD jets; at a later stage using Z decays in two leptons.
– Perform extensive measurements of SM processes at center-of-mass energy $\sqrt{s} = 7$ (or 10) TeV. The initial precision for cross-section measurements will be limited by systematic uncertainties, on acceptance, efficiency and luminosity, whose accuracy is expected to be $\sim$10%.

Whilst early data have an invaluable role to play in commissioning the detector, at the same time, physics measurements can be made in the first days even with a data sample of $\sim$1 pb^{-1}. Models of inclusive particle distributions with minimum-bias trigger, for example, make significantly different predictions, and few hours of data taking would provide adequate statistics to discriminate among them. With data samples of $\sim$100 pb^{-1}, accurate calibration and alignment will be obtained for all detectors and cross-sections measurements for Z, W, QCD jets, $t\bar{t}$ production become a realistic objective.
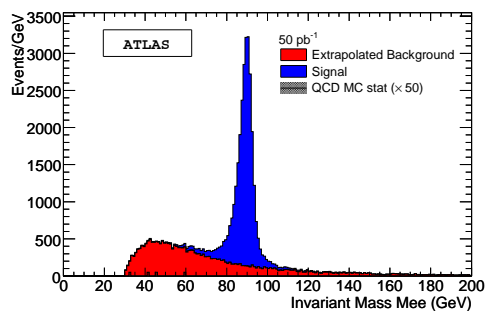
Fig. 12. Invariant mass distribution for $Z \rightarrow ee$ expected for an integrated luminosity of 50 pb^{-1}.
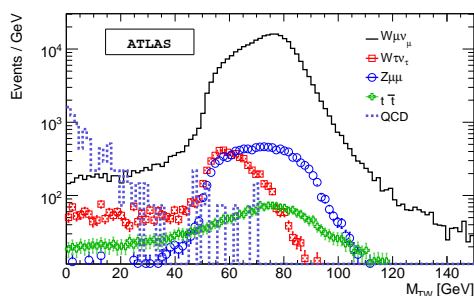
Fig. 13. Transverse mass distribution for $W \rightarrow \mu\nu$ events expected for an integrated luminosity of 50 pb^{-1}.

With 50 pb^{-1} the expected number of events for $Z \to \mu\mu$ and $Z \to ee$ (Fig. 12) is $\mathcal{O}(10^4)$ and for $W \to \mu\nu$ (Fig. 13) and $W \to e\nu$ is $\mathcal{O}(10^5)$. Cross-sections and inclusive distributions can be measured with statistical precision of a few percent. The Z leptonic decay is extremely useful to understand and improve the detector performance, in terms of calibrations, alignments, momentum, and energy scale. An example is represented by the "tag and probe" technique applied to Z events used to measure the MS local efficiency. Requiring two tracks in the ID with invariant mass close to m_Z, and at least one associated with a MS track (the "tag" muon), then the second ID track is extrapolated to probe an associated MS track. An integrated luminosity of $\sim$100 pb^{-1} is required to fully map the efficiency of the MS in 300 bins in η, ϕ, p_T, with 1–2% accuracy. However, a statistical precision of 1% for the average reconstruction efficiency can be reached with 1 pb^{-1}.

With a $t\bar{t}$ production cross-section of $\sim$830 pb at 14 TeV, LHC will be a top factory. About 500 events are expected in the decay channel to lepton–jet ($t\bar{t} \to bWbW \to bl\nu bjj$) with 100 pb^{-1} at 14 TeV (see Fig. 14). Even running at lower energy in the first year, the top signal will be observable with no b–tagging and simple analysis, and the cross-section will be measured with a statistical accuracy of $\sim$10%. This channel is of great interest since it contains all relevant signatures: electrons, muons, jets, missing transverse energy and b–jets, representing a benchmark for testing b–tagging algorithms and calibrating the jet energy scale with the $W \to jj$ invariant mass.
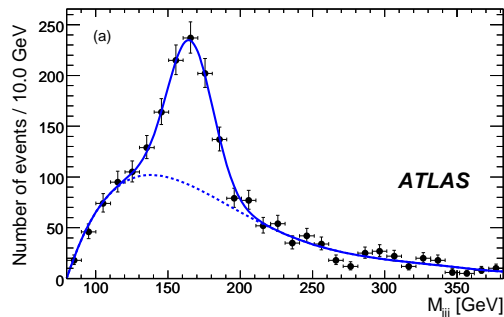

Fig. 14. Invariant mass distribution of the three jets associated to the top quark with 100 pb^{-1}.

4 Summary

To conclude, the ATLAS decector is well trained and well prepared for the highest energy proton collisions. At the time of writing these proceedings, November 2009, the LHC is undertaking the first collisions at 900 GeV in the center-of-mass energy. This event represents the "start of a fantastic era of physics and hopefully discoveries after 20 years' work by the international community to build a machine and detectors of unprecedented complexity and performance" as said by Fabiola Gianotti, the ATLAS spokeperson.

References

1. The ATLAS Technical Proposal, CERN-LHCC/94-43, 15.12.1994.
2. The ATLAS Collaboration, G. Aad et al., Expected Performance of the ATLAS Experiment: Detector, Trigger and Physics, CERN-OPEN 2008-020, December 2008, ISBN 978-92-9083-321-5.
3. The ATLAS Collaboration, G. Aad et al., *The ATLAS Experiment at the CERN Large Hadron Collider*, JINST **3**, S08003, 2008.
4. C. Adorisio et al. *System Test of the ATLAS Muon Spectrometer in the H8 Beam at the CERN SPS*, Nucl. Instrum. Meth. A 593, 232-254, 2008.